

ARTICLE

## Unravelling the Potential of Disposable and Modifiable Pencils as Catalyst Supports for Hydrogen Evolution Reaction

Received 00th January 20xx,  
Accepted 00th January 20xx

DOI: 10.1039/x0xx00000x

Mohan Paudel,<sup>a</sup> Braydan Daniels,<sup>b</sup> Amanda M. Arts,<sup>b</sup> Alexander Gupta,<sup>b,c</sup> Theodore Kalbfleisch,<sup>b</sup> Dillon T. Hofsommer,<sup>a</sup> Craig A. Grapperhaus,<sup>\*a</sup> Robert M. Buchanan,<sup>\*a</sup> Gautam Gupta<sup>\*b</sup>

**Abstract:** Increasing fossil fuel demands and growing concerns of global climate change have stimulated interest in the development of electrocatalysts to produce H<sub>2</sub> as an alternative zero-emission fuel from the electrolysis of water via hydrogen evolution reaction (HER). Precious or non-precious catalysts are typically loaded on high surface area carbon materials, and these supports play a critical role in both thermodynamics and kinetics of the HER. In this paper, we evaluate the electrocatalytic activity of a molecular hydrogen evolving catalyst, diacetyl-bis(4-methyl-3-thiosemicarbazone Ni(II)) (Ni-ATSM), on three different carbon surfaces: glassy carbon, carbon paste and pencil graphite. The overpotential for each modified electrode was benchmarked at a current density of -10 mA/cm<sup>2</sup>. Carbon paste electrodes showed highest overpotentials (495 mV) compared to the other electrode surfaces. Polished pencil and glassy carbon modified electrodes performed similarly ( $\eta = 395$  mV for GCE and  $\eta = 400$  mV for pencil). Pencil electrodes etched in acetone overnight prior to Ni-ATSM deposition produced lowest overpotentials ( $\eta = 354$  mV). Etching results in an increase in electroactive surface area and substantial decrease in the charge transfer resistance of the graphitic interface from 275  $\Omega$  to 50  $\Omega$ , verified using electrochemical impedance spectroscopy (EIS). Our studies demonstrate pencil graphite may serve as versatile, disposable, cost effective, and reproducible electrode surface for the evaluation of heterogeneous HER catalysts. Moreover, pencils can be easily cut with table saw to generate new surface for easy characterization of the surface such as electrochemistry, imaging and spectroscopy.

### Introduction

Fossil fuels remain the primary source of energy in the modern era and are depleting rapidly. Moreover, burning them at such a drastic rate has raised significant environmental concerns. Hydrogen is a promising alternative fuel with high specific energy, but currently nearly all hydrogen production is derived from fossil fuels.<sup>1</sup> Photovoltaic devices coupled with an electrolyser or direct water splitting can be used to generate an unlimited supply of hydrogen.<sup>2</sup> Hydrogen is generated electrochemically when sufficient potential is applied at the surface of an electrode.<sup>3</sup> The physical and chemical properties of the support material as well as the electrocatalyst properties directly impact both the thermodynamic and the kinetic parameters of the hydrogen evolution reaction (HER).<sup>4</sup> The HER

half-cell reaction theoretically should occur at 0.0 V vs normal hydrogen electrode (NHE).<sup>4</sup> However, to induce HER at an electrode surface, a higher potential (more negative) than 0.0 V must be applied (activation overpotential).<sup>3, 5</sup> Significant research on HER catalysts and supports has been conducted over last two decades to reduce the overpotential associated with HER. Several investigators have shown that platinum group metal (PGM) catalysts supported on carbon surfaces are the best HER catalysts reported to date,<sup>6-8</sup> but their use commercially remain cost prohibited. Recently, development of lower-cost PGM-free catalysts has constituted a major effort in energy conversion research.<sup>5, 9</sup> These materials typically require significant evaluation on inert carbon support materials to improve charge transfer and specify surface area.<sup>10</sup> Several forms of carbon including highly oriented pyrolytic graphite, glassy carbon, carbon fiber, boron-doped diamond, carbon paste, and carbon composites have been utilized as supporting electrodes to evaluate the performance of non-precious catalysts.<sup>11-16</sup> For several decades, glassy carbon electrodes (GCE) have been utilized primarily as the supporting electrode material in the *ex-situ* characterization of novel catalysts due to its chemical inertness, well defined surface area, good electrical conductivity, and stability.<sup>17</sup> However, GCE is non-disposable,

<sup>a</sup> Department of Chemistry, University of Louisville  
2320 South Brook Street, Louisville, Kentucky 40292, USA.

<sup>b</sup> Conn Centre for Renewable Energy Research, University of Louisville  
Louisville, Kentucky 40292, USA.

<sup>c</sup> Los Alamos National Laboratory  
Los Alamos, New Mexico 87545, USA.

Electronic Supplementary Information (ESI) available: [details of any supplementary information available should be included here]. See DOI: 10.1039/x0xx00000x

expensive, requires extensive cleaning and polishing between tests. More importantly, in some cases GCE surfaces are not amenable for post-characterization as they are sealed in a Teflon or PEEK sleeve. Replaceable GCE tips can be purchased, but they are extremely expensive. All of these issues can severely impact the high throughput electrochemical analysis of materials for applications in catalysis, sensing, corrosion, and others. Another frequently used electrode is the carbon paste electrode (CPE),<sup>18</sup> which is straightforward to fabricate and can be easily characterized.<sup>19</sup> Interestingly, despite its significant expense, the GC electrode - essentially a cylinder of sp<sup>2</sup>-hybridized carbon - is very similar to the common graphite pencil, which is readily available, inexpensive, disposable, and amenable to post-characterization. Modified pencils have been used as electrodes for electrochemical sensing and determination of different metal ions, molecules, enzymes and drugs for a while in the past.<sup>20-23</sup> Mercury coated pencil electrodes were used by Bond *et al.* for the detection of lead, cadmium and uranium using stripping voltammetry.<sup>24</sup> Pencils electrodes also have been modified using electrodeposition to study HER activity of various catalysts.<sup>25, 26</sup> To the best of our knowledge a comprehensive comparative study of pencil electrodes in HER catalysis has not been reported.

The focus of this study is to (a) compare the HER activity of pencils with different hardness and graphite contents (HB, 2B, 4B, 8B)<sup>27, 28</sup> to the activity of CPE and GCE; (b) evaluate and compare the electrochemical performance of a well-studied HER catalyst on HB pencils, CPEs and GCEs; and (c) develop simple procedures that can modify the carbon support through mild solvent treatment to enhance the electrochemical performance of the catalyst. Specifically, herein we compare the electrocatalytic activity of a known homogeneous hydrogen evolving catalyst, diacetyl-bis(4-methyl)-3-thiosemicarbazone Ni(II) (Ni-ATSM), drop casted on: glassy carbon, carbon paste, HB pencil graphite, and acetone etched HB pencil graphite electrodes using linear sweep voltammetry (LSV). HB pencils and modified pencil electrodes are shown to behave as versatile catalyst supports for HER compared to glassy carbon electrodes as a result of their low cost, general availability, ease of surface generation, and characterization.

## Experimental Section

### Materials and Methods.

All chemicals and solvents were used as purchased from commercial sources unless otherwise indicated. The molecular structure and purity of the Ni-ATSM catalyst was confirmed by <sup>1</sup>H NMR (Varian Inova 500 MHz Spectrometer) in commercial deuterated DMSO-D<sub>6</sub> (Cambridge Isotopes). UV-visible spectra were obtained using an Agilent 8453 diode array spectrophotometer and a quartz cuvette with 1cm path length. IR spectra were recorded using a Thermo Scientific Nicolet iS20 spectrometer equipped with smart iTR. Surface characterization after deposition of catalyst ink was done using a TESCAN VEGA3 scanning electron microscope (SEM) operating at 10 kV and 10 mA. Raman spectra were collected using a Reva

Educational Raman spectrometer (Hellma USA, Inc., Plainview, NY). BRUKER Discovery D8 HR-XRD was used to collect XRD spectra. Electrochemical characterization (ECC) methods include linear sweep voltammetry (LSV), cyclic voltammetry (CV), and electrochemical impedance spectroscopy (EIS). A Metrohm Autolab PGSTAT302N potentiostat was used for ECC in a three-electrode glass electrochemical cell (RDE/RRDE Cell Without Water Jacket, Pine Research). Where noted, a glassy carbon electrode was used as the working electrode in 0.5 M H<sub>2</sub>SO<sub>4</sub> (VWR, ACS grade) solution prepared with twice-deionized Millipore water (18.2 Ω cm). A graphite rod (Pine Research), in a protective fritted glass tube (Pine Research), was used as the counter electrode. Ag/AgCl (1 M KCl, CH Instruments) was used as the reference electrode. High-purity N<sub>2</sub> gas used throughout these experiments was supplied from Welders Supply, Louisville, KY.

### Electrode Preparation.

Rotating disc glassy carbon electrodes purchased from Pine Research were sonicated in ethanol and DI water for 15 minutes and then polished using an alumina slurry prior to each electrochemical study. Electrochemical cleaning was further performed by cycling from 1.2 V to -1.2 V for 20 cycles. Finally, the electrodes were tested with ferricyanide solution to verify the cleaning procedure, and thoroughly rinsed with water and air dried prior to drop casting of the catalyst ink. Carbon paste electrodes (CPE) were fabricated using literature methods.<sup>29</sup> Graphite powder was mixed with paraffin oil in the 8:2 ratio by weight and mixed thoroughly by mortar and pestle. The prepared carbon paste was filled in the carbon paste holder from BASI Research products. Surface of carbon paste was smoothed using weighing paper and air dried at room temperature prior to drop casting of the catalyst ink. Ticonderoga number HB, 4B and 8B pencils were used as a substrate for evaluating the electrochemical activity of the catalysts. Pencils were sliced using a tabletop diamond edge saw to generate clean flat surfaces and referred to as 'blank pencil', while the other end was sharpened to expose a graphite tip for electrical contact. Catalyst inks were drop casted on all surfaces and subsequently used to evaluate their respective HER activity. HB pencil surfaces were further modified to enhance the surface area of the substrate. Specifically, HB pencils were etched with acetone overnight to remove any soluble organic clays and binding materials from the surface. This modified surface is referred to as 'etched pencil' for loading catalyst inks. A fresh surface was easily created by cutting the same pencil again with a tabletop diamond edged saw to continue the studies on the same pencil. CPE, PGE and GCE were characterized by FT-IR and XRD as shown in Figure S1.

### Catalyst Synthesis and Characterization.

Ni-ATSM was used as a model catalyst for the HER studies. The ligand H<sub>2</sub>ATSM was synthesized and metallated with nickel acetylacetonate to obtain Ni-ATSM following a previously reported procedure.<sup>30, 31</sup> The catalyst was characterized using <sup>1</sup>H NMR, FT-IR and UV-visible spectroscopy (Figure S2 and S3).

**Catalyst Ink Preparation and Loading.**

Catalyst inks were prepared by dispersing 4 mg/mL Ni-ATSM in 4:1 v/v H<sub>2</sub>O/ethanol and adding 40  $\mu$ L 10% Nafion solution, which acts as a binding agent. Prior to deposition, inks were homogenized via ultrasonication and drop casted (0.285 mg/cm<sup>2</sup> catalyst) on the surface of the electrode then air dried before conducting measurements. The resulting electrodes were studied for HER activity using linear sweep voltammetry and the resistance of the deposited films were measured using EIS.

**HER Activity of Modified Electrodes.**

Reductive cycling between 0 to -0.8 V versus reversible hydrogen electrode (RHE) at scan rate of 50 mV/s was used to condition the modified electrode surfaces. LSV and EIS were performed over the same potential range before conditioning of electrode and after every 100 reductive cycles to evaluate the activity of the catalyst. The EIS measurements were conducted at -0.3 V vs RHE to determine the impedance of the working electrode of the cell by reducing the frequency from 100,000 Hz to 0.02 Hz.<sup>32</sup> Polarization curves and impedance measurements are reported at the peak reductive cycling (300-500 cycles).

**Quantitative Hydrogen Evolution Monitoring.**

H<sub>2</sub> evolution was confirmed using a H-cell fitted with a gas-tight "low-volume cap" (Pine Research) containing an Ag/AgCl reference, gas dispersion tube, gas outlet, and the working electrode of interest. The Pt mesh counter electrode was separated by a Nafion 115 membrane, and each side was filled with 0.5 M H<sub>2</sub>SO<sub>4</sub>. Chronopotentiometry at -10 mA cm<sup>-2</sup> (Figure S15) was performed for 120 minutes while nitrogen gas was fed into the cell at 5 sccm. 1 mL of gas was sampled every 10 minutes by an in-line gas chromatographer (SRI Instrument, Multiple Gas Analyzer #1 + Sulfur), and the faradaic efficiency was quantified by comparing H<sub>2</sub> production from the electrode against a Pt electrode under the same current and gas flow rate.

values and Tafel slopes for all the carbon supports are reported in Table S1. Figure 1b shows the Tafel plots of all the carbon electrodes evaluated during HER. GCE and CPE have lower Tafel slopes than the different grade of pencils indicating faster electron transfer kinetics.

Figure S5 shows the Nyquist plots for the pencil electrodes which clearly shows decreasing charge transfer resistance for pencils as the graphite content is increased (where 8B < 4B < HB). In contrast, the GCE has the highest charge transfer resistance. The low charge transfer resistance of the pencils may be attributed to the presence of several edge defects in comparison to the polished GCE electrode which has a more atomically flat surface.

GCEs are not only expensive but require significant time-consuming cleaning and polishing steps. In contrast, PGEs offer significant advantages over GCEs as they are inexpensive and can be used as disposable electrodes. Figure S6 shows PGE surfaces can be cut allowing for post-electrolysis characterization and the newly exposed surface behaves qualitatively similar to the original surface. Stability of PGE was evaluated using reductive CV cycling. As displayed in the LSV plot in Figure S7 there is relatively small difference in overpotential of blank pencil after 1000 reductive cycling. We can see from the LSV plots that HB pencils are as stable a carbon support as glassy carbon for catalysts. Although the electrochemical activity and variability of the PGE is slightly higher than both CPE and GCE, they are still relatively inert as all of the electrodes exhibit significantly higher overpotentials than HER catalysts and therefore can be used as substrates to evaluate the performance of precious or non-precious electrocatalysts.

## Results and Discussion

**Electrochemical evaluation of carbon supports.**

The electrochemical performance of several carbon substrates: GCE, CPE, and different grades of pencil graphite electrodes (PGE) were evaluated. Figure 1a shows the linear sweep voltammetry and Figure S4 shows cyclic voltammetry data for all carbon supports employed in the study. For ease of comparison, overpotentials were determined using -10 mA/cm<sup>2</sup> as a benchmark current density.<sup>33, 34</sup> LSV data indicate GCE and CPE have the highest overpotentials out of the carbon substrates studied herein, indicating extremely inert surfaces (low current density at high overpotentials). The overpotential for a GCE is more than 0.9 V. In contrast, the PGE electrodes show higher electrochemical activity and have a lower overpotential of around 0.75 V. All PGE electrodes displayed similar performance as shown in Figure 1a. The overpotential

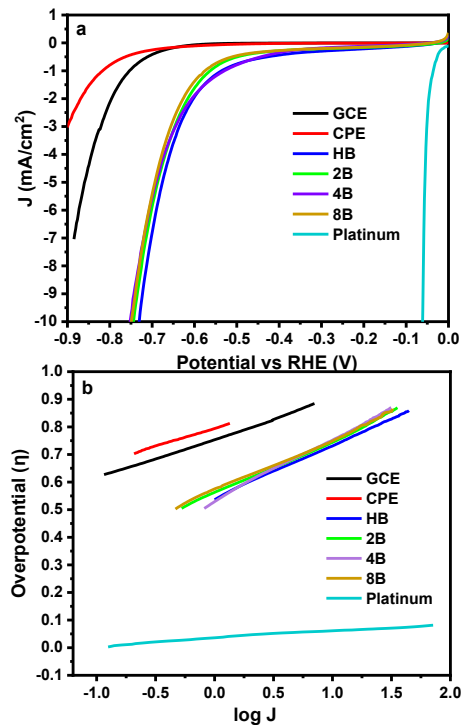


**Fig. 1.** HER performance of various carbon supports following reductive cycling at peak catalytic activity in 0.5 M H<sub>2</sub>SO<sub>4</sub>. (a) LSV plots for various carbon supports with overpotential determined at current density of -10 mA/cm<sup>2</sup>. (b) Tafel plots showing current response to increasing overpotential throughout onset period.

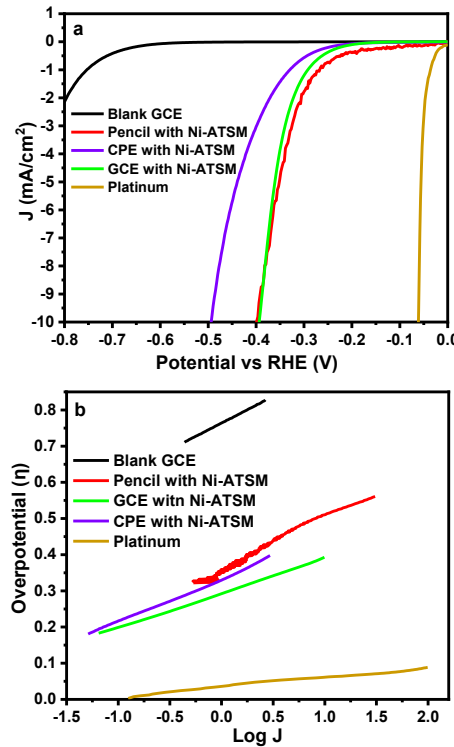
#### Electrochemical performance of Ni-ATSM inks on carbon substrates.

GCE, CPE, and PGE were prepared and cleaned as reported in the experimental section, and surface modified electrodes were prepared by drop casting Ni-ATSM inks. Figure 2a shows LSV plots for an unmodified GCE and platinum wire in comparison with all other substrates with catalysts inks. As expected, there is a large drop in overpotential of HER for all of the carbon electrodes with surface deposited catalyst compared to the bare carbon surfaces. The overpotential for a surface modified CPE is 0.493 V, whereas for surface modified GCE, the overpotential is 0.395 V. A previous study by Gupta *et al.*<sup>32</sup> showed a similar decrease in overpotential for NiATSM deposited on GCE after reductive cycling. Surface modified PGE electrodes showed overpotentials near 0.4 V, similar to GCE. Figure S9 also compares LSV and Tafel plots of carbon supports with and without catalyst. Decrease in both the overpotential and Tafel slope was observed after addition of catalyst on the carbon surface which shows good catalytic activity of Ni-ATSM for HER on all carbon supports. Cyclic voltammograms of

different carbon substrates with Ni-ATSM are also shown in Figure S10. Figure 3b shows the Tafel slopes for the respective electrodes modified by the catalyst ink. Slope values are reported in the Table S2. The data indicate an increase in electron transfer kinetics after drop casting the catalyst ink on the carbon support. According to Butler-Volmer kinetics when the Tafel slope is near 118 mV/dec, the Volmer step is the rate determining step of the HER.<sup>35</sup> Surface modified GCE showed a Tafel slope of 90 mV/dec, while the CPE and PGE showed slopes of 118 mV/dec and 137 mV/dec respectively.

As mentioned above, the glassy carbon electrode has a smooth surface and hence has the same electrochemically active surface as its geometric surface. In contrast the presence of paraffin (binder) in CPE can limit electrolyte accessibility to the carbon surface and thus lowering its electrochemical activity. Pencils on the other hand, offer electrochemical activity similar to GCE even in the presence of silica and binder materials, although they display higher Tafel slopes.

One criticism of pencil electrodes is that the surface is non-uniform from electrode to electrode, so it is expected that measurements might have slightly low reproducibility. However, both PGE and GCE surfaces are modified in terms of active surface area when drop



casted with catalyst. Figure 3 shows several instances of catalyst drop casted PGEs and GCEs. Importantly, there is nearly the same

variance in PGE as in GCE, and all overpotentials lie within 50 mV of one another. Catalyst modified PGEs therefore gives reproducible data which matches to that of GCE while being disposable. The catalyst modified surface can thus be easily separated from the pencil for post-electrolysis materials characterization techniques like SEM or even more destructive methods without sacrificing an expensive electrode.

Fig. 2. Comparative a) LSV and b) Tafel of Blank GCE, HB pencil with catalyst, CPE with catalyst, GCE with catalyst at peak reductive cycling with platinum.

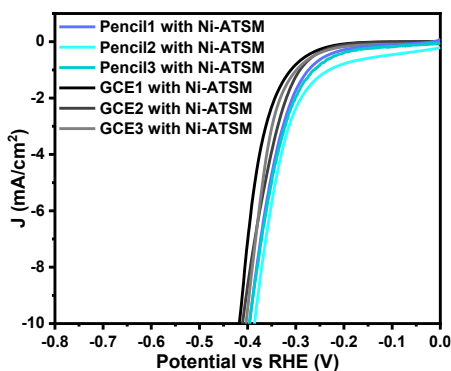
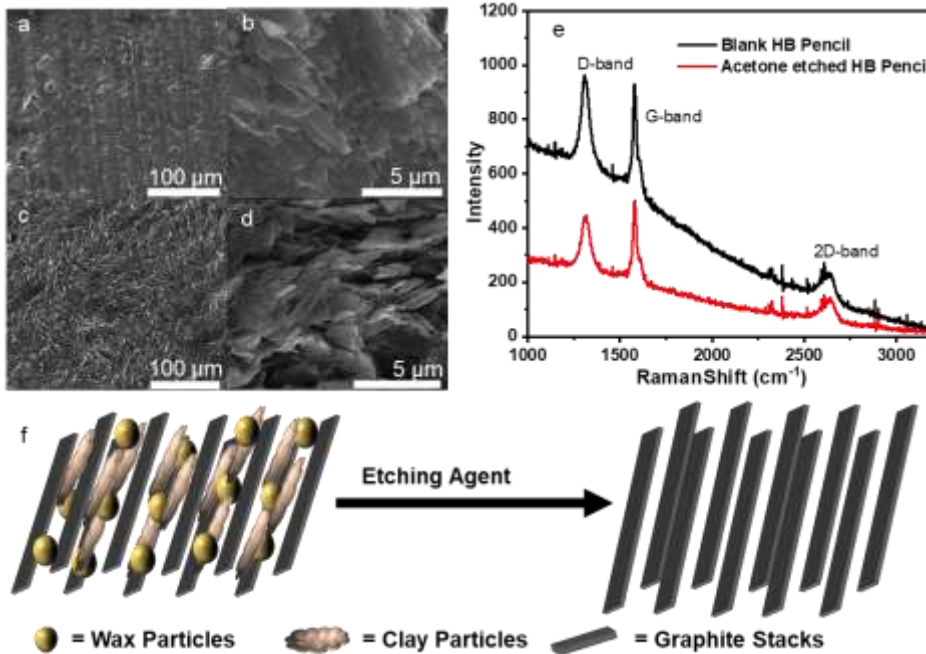


Fig. 3. LSV of multiple Ni-ATSM modified GCE (gray scale) and pencil surface (blue).



**Commented [GC1]:** In H<sub>2</sub>SO<sub>4</sub>, right? This needs to be in caption

and catalyst loading resulting in an increase in catalytic activity.

Figure 4e shows the Raman spectra of a HB pencil before and after etching. The Raman shifts at  $1310\text{ cm}^{-1}$  (D-band),

Fig. 4 SEM images of (a,b) unetched HB pencil and (c,d) acetone etched HB pencil and (e) Raman spectra of the same PGEs f) Schematic representation of vacancy generation in pencil graphite after etching.

$1580\text{ cm}^{-1}$  (G-band) and  $2640\text{ cm}^{-1}$  (2D-band) were observed for both unetched and etched pencils. The G-band is associated with  $\text{sp}^2$  carbon of graphitic sheets. The intensity of 2D-band is associated with the thickness of the graphitic layers whereas the D-band is associated with the defects or disorder of the graphene sheets.<sup>37,38</sup> A decrease in the relative intensity of the D-band (decrease in  $I_D/I_G$  ratio from 0.79 to 0.73) was observed after acetone etching. This indicates there is a decrease in defects of graphitic layers, which results from the removal of the binder. Figure 4f shows a schematic representation of acetone etching of (overnight dipping) the pencil surface, removing the binder agents. These results clearly indicate improvement in the quality of graphite content after etching. Electrochemical performance of the NiATSM modified pencil electrode is shown in Figure 5. LSV plots for a HB pencil before and after acetone etching show a dramatic change in overpotential associated with the etched pencil. The acetone etched pencil showed much lower overpotential for HER compared to the unetched pencil. Before etching the overpotential was observed to be 0.78 V, and after etching it decreased to 0.60 V. This decrease in overpotential after etching implies an increase in graphite surface area as a result of etching. Impedance measurements (Figure S12) confirm these results. There is a substantial decrease in the charge transfer resistance of the graphite interface from  $275\text{ }\Omega$  to  $50\text{ }\Omega$  after acetone etching. However, the Tafel slope of etched pencil does not change significantly compared to the unetched pencil. Capacitance measurements were performed to compare the electrochemical surface area (ECSA) of an etched pencil and unetched pencil. After etching, the integrated current measured in the same potential window of the cyclic voltammogram doubled in comparison to the unetched pencil. Area of integrated current can be related directly to the surface area of the electrode. Therefore, the results show the active surface area of pencil graphite doubled after etching (Table S3). When correction in active surface area of etched pencil is applied in the polarization curve, it overlaps with the polarization curve of an unetched pencil (Figure S13) implying improvement in HER activity is based on an increase in the active surface area of the pencil graphite after etching.

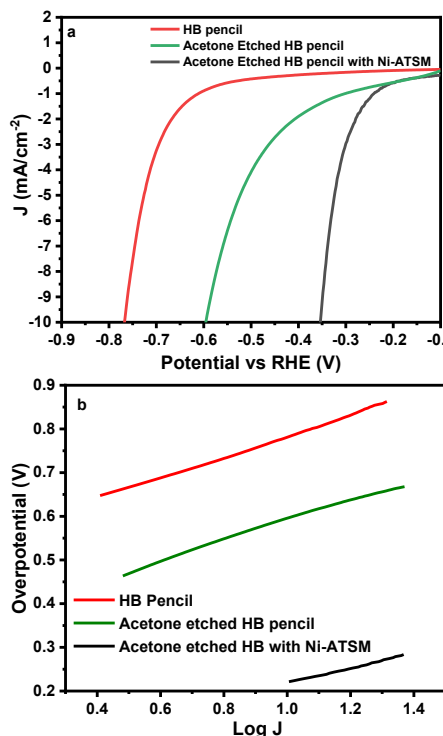


Fig. 5. LSV and Tafel of Pencil with catalyst before and after etching with acetone.

NiATSM ( $0.285\text{ mg/cm}^2$  of catalyst) was drop casted on the surface of an etched pencil and LSV and EIS measurements were conducted. This electrode could be cleaned by sonication in acetone to leach out the catalyst and regenerate the original unmodified surface as shown in Figure S14. The modified acetone etched pencil displayed a lower overpotential of  $0.354\text{ V}$  at a current density of  $-10\text{ mA/cm}^2$  (Figure 5a), which is a  $50\text{ mV}$  drop in HER overpotential. We also observed a decrease in the Tafel slope from  $137\text{ mV/dec}$  for the unetched Ni-ATSM modified PGE electrode to  $116\text{ mV/dec}$  for the Ni-ATSM modified acetone etched electrode. Hydrogen was produced at essentially  $100\%$  faradaic efficiency (Table S4) from both NiATSM-modified and unmodified acetone etched pencils as quantified by gas chromatography. Thus, the higher activity in both cases is not due to reduction of any contaminants. Instead, the changes in Tafel slope upon etching suggest an improvement in electron transfer kinetics between the surface

confined catalyst and the etched electrode surface. The lower overpotential and Tafel slope upon acetone etching arises due to the increase of ECSA of the PGE. Acetone etching of pencil electrodes is therefore a simple technique for increasing the sensitivity of modified or unmodified PGEs.

## Conclusion

In this study we compared the HER activity of a model molecular HER active Ni-ATSM catalyst on three different carbon supports GCE, PGE, and CPE. We demonstrate that the HB pencil is a viable disposable carbon support that can be used to study HER catalysts in a comparable manner to GCEs. Furthermore, the etching of pencil utilizing acetone enhances the surface area of the carbon support and the electroactivity of the catalyst can be further improved. By utilizing the methods mentioned above, researchers studying new materials for the HER or other reactions will be able to characterize catalysts in a reliable and a relatively quick way in contrast to using GCEs thus paving a path to accelerated development of new materials. Also, utilization of pencil electrodes can simplify post-electrochemical surface characterization compared to GCE. Moreover, developing of new etching methods can further enhance the active surface area of carbon supports and can be a valuable tool for sensing and catalytic processes.

## Acknowledgements

The authors wish to acknowledge Sashil Chapagain from University of Louisville for help collecting XRD spectra and Meenakshi Bansal from Thomas Moore University for help collecting Raman spectra.

## Funding Sources

This work was supported by NSF grant number CHE-1800245 and CHE-1955268

## Author Contributions

The manuscript was written through contributions of all authors. All authors have given approval to the final version of the manuscript.

## Conflicts of interest

There are no conflicts to declare.

## Notes and references

1. F. Birol, *Journal*, 2019.
2. A. Turner John, *Science*, 2004, **305**, 972-974.
3. X. Zou and Y. Zhang, *Chem Soc Rev*, 2015, **44**, 5148-5180.
4. Y. Jiao, Y. Zheng, M. Jaroniec and S. Z. Qiao, *Chem Soc Rev*, 2015, **44**, 2060-2086.
5. J. D. Benck, T. R. Hellstern, J. Kibsgaard, P. Chakraborty and T. F. Jaramillo, *ACS Catalysis*, 2014, **4**, 3957-3971.
6. W. Sheng, H. a. Gasteiger and Y. Shao-Horn, *Journal of The Electrochemical Society*, 2010, **157**, B1529-B1529.
7. N. Dubouis and A. Grimaud, *Chemical Science*, 2019, **10**, 9165-9181.
8. R. D. Giles, J. A. Harrison and H. R. Thirsk, *Journal of Electroanalytical Chemistry and Interfacial Electrochemistry*, 1969, **20**, 47-60.
9. Z. W. Seh, J. Kibsgaard, C. F. Dickens, I. Chorkendorff, J. K. Norskov and T. F. Jaramillo, *Science*, 2017, **355**.
10. D. Voiry, R. Fullon, J. Yang, E. S. C. de Carvalho Castro, R. Kappera, I. Bozkurt, D. Kaplan, M. J. Lagos, P. E. Batson, G. Gupta, A. D. Mohite, L. Dong, D. Er, V. B. Shenoy, T. Asefa and M. Chhowalla, *Nat Mater*, 2016, **15**, 1003-1009.
11. G. Girishkumar, M. Rettker, R. Underhill, D. Binz, K. Vinodgopal, P. McGinn and P. Kamat, *Langmuir*, 2005, **21**, 8487-8494.
12. E. Guilminot, F. Fischer, M. Chatenet, A. Rigacci, S. Berthon-Fabry, P. Achard and E. Chainet, *Journal of Power Sources*, 2007, **166**, 104-111.
13. N. Rajalakshmi, H. Ryu, M. M. Shajumon and S. Ramaprabhu, *Journal of Power Sources*, 2005, **140**, 250-257.
14. G. Siné, I. Duo, B. E. Roustom, G. Fóti and C. Comninellis, *Journal of Applied Electrochemistry*, 2006, **36**, 847-862.
15. H. Remita, P. F. Siril, I.-M. Mbomekalle, B. Keita and L. Nadjo, *Journal of Solid State Electrochemistry*, 2005, **10**, 506.
16. T. Brüll and U. Stimming, *Journal of Electroanalytical Chemistry*, 2009, **636**, 10-17.
17. H. E. Z. a. F. J. Miller, *Analytical Chemistry*, 1965, **37**, 200-203.
18. R. N. J. A. c. Adams, 1958, **30**, 1576-1576.
19. A. Abbaspour and E. J. F. Mirahmadi, 2013, **104**, 575-582.
20. Annu, S. Sharma, R. Jain and A. N. Raja, *Journal of The Electrochemical Society*, 2019, **167**, 037501.
21. C. Guo, C. Chen, Z. Luo and L. Chen, *Analytical Methods*, 2012, **4**, 1377-1382.
22. N. Oyama and F. C. J. J. o. t. A. C. S. Anson, 1979, **101**, 3450-3456.
23. J. I. Gowda and S. T. J. E. A. Nandibewoor, 2014, **116**, 326-333.
24. P. J. M. Alan M. Bond, Jorg Schiwe, Victoria Vicente-Beckett, *Analytica Chimica Acta*, 1997, **345**, 67-74.
25. S. Pourbeyram, M. Ranjbar and M. Soltanpour, *Journal of the Iranian Chemical Society*, 2019, **16**, 2065-2070.
26. D. Balun Kayan and D. J. J. o. S. S. E. Koçak, 2017, **21**, 2791-2798.
27. *United States Pat.*, 5118345, 1992.
28. R. V. N. R.N. Bhowmik, Kalapet, *Ferromagnetism in lead graphite-pencils and magnetic composite with CoFe2O4 particles*, Department of Physics, Pondicherry University.
29. H. Beitollahi, A. Gholami, M. R. J. M. S. Ganjali and E. C, 2015, **57**, 107-112.
30. S. Gulati, O. Hietsoi, C. A. Calvary, J. M. Strain, S. Pishgar, H. C. Brun, C. A. Grapperhaus, R. M. Buchanan and J. M. Spurgeon, *Chemical Communications*, 2019, **55**, 9440-9443.

Please do not adjust margins

ARTICLE

Journal Name

31. D. X. West, J. S. Ives, G. A. Bain, A. E. Liberta, J. Valdés-Martínez, K. H. Ebert and S. Hernández-Ortega, *Polyhedron*, 1997, **16**, 1895-1905.
32. A. J. Gupta, N. S. Vishnosky, O. Hietsoi, Y. Losovýj, J. Strain, J. Spurgeon, M. S. Mashuta, R. Jain, R. M. Buchanan, G. Gupta and C. A. Grapperhaus, *Inorganic Chemistry*, 2019, **58**, 12025-12039.
33. M. G. Walter, E. L. Warren, J. R. McKone, S. W. Boettcher, Q. Mi, E. A. Santori and N. S. J. C. r. Lewis, 2010, **110**, 6446-6473.
34. M. F. Weber and M. J. J. J. o. T. E. S. Dignam, 1984, **131**, 1258.
35. M. Zeng and Y. Li, *Journal of Materials Chemistry A*, 2015, **3**, 14942-14962.
36. M. C. Sousa and J. W. Buchanan, *Computer Graphics Forum*, 2000, **19**, 27-49.
37. Y. Lei, A. H. Alshareef, W. Zhao and S. Inal, *ACS Applied Nano Materials*, 2020, **3**, 1166-1174.
38. R. Navratil, A. Kotzianova, V. Halouzka, T. Opletal, I. Triskova, L. Trnkova and J. Hrbac, *Journal of Electroanalytical Chemistry*, 2016, **783**, 152-160.

Please do not adjust margins